The inherent multidimensionality of temporal variability: how common and rare species shape stability patterns

Jean-François Arnoldi, Michel Loreau, Bart Haegeman

The inherent multidimensionality of temporal variability: How common and rare species shape stability patterns

Jean-François Arnoldi[1,2,*], Michel Loreau[1], and Bart Haegeman[1]

[1] *Centre for Biodiversity Theory and Modelling, Theoretical and Experimental Ecology Station, CNRS and Paul Sabatier University, 09200 Moulis, France.*

[2] *Zoology department, School of Natural Sciences, Trinity College Dublin, The University of Dublin, Ireland.*

[*] *arnoldij@tcd.ie.*

June 7, 2019

Statement of authorship: JFA and BH developed the theory and performed numerical simulations. JFA wrote the first draft of the manuscript, and ML and BH contributed substantially to revisions.

Data accessibility statement: This work does not use data. Matlab simulation code is available online (bioRxiv server) DOI: 10.1101/431296 (supplementary material).

Running title: The inherent multidimensionality of variability.

Type of article: Letters.

Keywords: diversity-stability relationship, immigration stochasticity, demographic stochasticity, environmental stochasticity, rare species, common species, asymptotic resilience.

Number of words in abstract: 148.

Number of words in main text: 4769.

Number of references: 42.

Number of figures, tables and boxes: 6, 0, 0.

Abstract

Empirical knowledge of diversity-stability relationships is mostly based on the analysis of temporal variability. Variability, however, often depends on external factors that act as disturbances, which makes comparisons across systems difficult to interpret. Here we show how variability can reveal inherent stability properties of ecological communities. This requires abandoning one-dimensional representations, in which a single variability measurement is taken as a proxy for how stable a system is, and instead consider the whole set of variability values generated by all possible stochastic perturbations. Furthermore, in species-rich systems, a generic pattern emerges from community assembly, relating variability to the abundance of perturbed species. The contrasting contributions of different species abundance classes to variability, driven by different types of perturbations, can lead to opposite diversity-stability patterns. We conclude that a multidimensional perspective on variability helps reveal the dynamical richness of ecological systems and the underlying meaning of their stability patterns.

Introduction

Ecological stability is a notoriously elusive and multifaceted concept (Pimm, 1984; Donohue *et al.*, 2016). At the same time, understanding its drivers and relationship with biodiversity is a fundamental, pressing, yet enduring challenge for ecology (Elton, 1946; MacArthur, 1955; May, 1973a; McCann, 2000). The temporal variability of populations or ecosystem functions, where lower variability is interpreted as higher stability, is an attractive facet of ecological stability, for several reasons. First, variability is empirically accessible using simple time-series statistics (Tilman *et al.*, 1996). Second, variability – or its inverse, invariability – is a flexible notion that can be applied across levels of biological organization (Haegeman *et al.*, 2016) and spatial scales (Wang & Loreau, 2014; Wang *et al.*, 2017). Third, variability can be indicative of the risk that an ecological system might go extinct, collapse or experience a regime shift (Scheffer *et al.*, 2009). During the last decade, the relationship between biodiversity and ecological stability has thus been extensively studied empirically using invariability as a measure of stability (Tilman *et al.*, 2006; Jiang & Pu, 2009; Hector *et al.*, 2010; Campbell *et al.*, 2011; Gross *et al.*, 2014; Pennekamp *et al.*, 2018).

In a literal sense, stability is the property of what tends to remain unchanged (Pimm, 1991). Variability denotes the tendency of a variable to change in time, so that its inverse fits this intuitive definition. However, variability is not necessarily an inherent property of the system that is observed (e.g., a community of interacting species), as it typically also depends on external factors that act as perturbations. Thus, the variability of a community is not a property of that community *alone*. It may be caused by a particular perturbation regime so that a different regime could lead to a different value of variability. Stronger perturbations will generate larger fluctuations, and the way a perturbation's intensity is distributed and correlated across species is also critical. In other words, a variability measurement reflects

the response of a system to the specific environmental context in which it is embedded.

Despite this complexity, quantifying the fluctuations of an ecosystem property (e.g., primary production) can be of foremost practical interest as it provides a measure of predictability in a given environmental context (Griffin *et al.*, 2009). However, to generalize results beyond the specific context in which variability is measured, use variability to compare the stability of different systems, establish links between different stability notions, or reconcile the conflicting diversity-stability patterns and predictions reported in the empirical and theoretical literature (Ives & Carpenter, 2007), one needs to know how variability measurements can reflect a system's inherent dynamical features.

Here, we adopt an approach in which stability is viewed as the inherent ability of a dynamical system to endure perturbations (Fig. 1A). For simplicity we will restrict to systems near equilibrium, by opposition to, e.g., limit cycles or chaotic attractors. We propose that a measure of stability should reflect, not a particular perturbation (as in Fig. 1B), but a system's propensity to withstand *a whole class* of perturbations. We therefore consider a vast perturbation set, and study the corresponding range of community responses (Fig. 1C). Even from a theoretical perspective, considering all possible perturbations that an ecosystem can face is a daunting task. We will thus restrict our attention to communities near equilibrium, perturbed by stochastic perturbations, and derive analytical formulas for two complementary features of the set of their variability values: its average and maximum, corresponding to the mean- and worst-case perturbation scenarios, respectively. Our work follows traditional approaches of theoretical ecology (May, 1973a; Ives *et al.*, 2003), extending the analysis to encompass a large perturbation set.

After having developed a general theory of variability that can be applied to any system near equilibrium, we turn our attention to species-rich communities assembled from nonlinear dynamics. We show that a generic variability-abundance pattern emerges from the complex

interactions between species during assembly. We argue that this pattern, in conjunction with the type of perturbations considered (environmental, demographic, or caused by stochastic immigration), determines the specific species abundance class that governs the variability distribution. In particular, we establish a fundamental link between rare species, worst-case variability, and asymptotic resilience – the long-term rate of return to equilibrium following a pulse perturbation. We finally illustrate that the contrasting contributions of various species abundance classes can be responsible for opposite diversity-invariability patterns.

Material and Methods

Perturbed communities

Let $N_i(t)$ represent the abundance (or biomass) of species i at time t, and $x_i(t) = N_i(t) - N_i$ its displacement from an equilibrium value N_i, with i running over S coexisting species that form an ecological community. We model variability as a response to stochastic forcing. We focus on stationary fluctuations caused by weak perturbations with zero mean, governed by the following dynamical system, written from the perspective of species i as

$$\frac{d}{dt} \underbrace{x_i(t)}_{\text{fluctuations}} = \sum_{j=1}^{S} \underbrace{A_{ij} x_j(t)}_{\text{interactions}} + \underbrace{\sigma_i \sqrt{N_i}^{\alpha} \xi_i(t)}_{\text{perturbation}}. \tag{1}$$

The coefficients A_{ij} represent the effect that a small change of abundance of species j has on the abundance of species i. Organized in the *community matrix* $A = (A_{ij})$, they encode the linearization of the nonlinear system of which (N_i) is an equilibrium. In the perturbation term, $\xi_i(t)$ denotes a standard white-noise source (Arnold, 1974; Van Kampen, 1997). In discrete time $\xi_i(t)$ would be a normally distributed random variable with zero mean and unit

variance, drawn independently at each time step (Appendix 1).

Such models were studied by Ives *et al.* (2003) to analyze ecological time series. In their approach, stability properties are inferred from the system's response to specific perturbations. Here we build on a similar formalism, but explicitly explore a vast set of possible perturbations. Although environmental fluctuations often follow temporal patterns (Vasseur & Yodzis, 2004; Ruokolainen *et al.*, 2009; Fowler & Ruokolainen, 2013) we will not consider autocorrelated perturbations. What we will explicitly consider, however, are temporal correlations between $\xi_i(t)$ and $\xi_j(t)$, a situation in which individuals of species i and j are similar in their perception of a given perturbation, a property known to have potentially strong, and unintuitive effects on species dynamics (Ripa & Ives, 2003).

For the fluctuations of species abundance in eq. (1) to be stationary, the equilibrium state (N_i) must be stable. More technically, the eigenvalues of the community matrix A must have negative real part (May, 1973a; Gurney & Nisbet, 1998). The maximal real part determines the slowest long-term rate of return to equilibrium following a pulse perturbation. This rate is a commonly used stability measure in theoretical studies; we call it *asymptotic resilience* and denote it by $\mathcal{R}_\infty$ (Arnoldi *et al.*, 2016). To illustrate the connections between stability concepts, we will compare asymptotic resilience to measures of variability.

Perturbation type

The perturbation term in eq. (1) represents the direct effect that a perturbation has on the abundance of species i. It consists of two terms: some power α of $\sqrt{N_i}$, and a species-specific term $\sigma_i\xi_i(t)$. The latter is a function of the perturbation itself, and of traits of species i that determine how individuals of that species perceive the perturbation. The former defines a statistical relationship between a perturbation's direct effects and the mean abundance of

perturbed species. It allows us to consider ecologically distinct sources of variability (Fig. 2).

When individuals of a given species respond in synchrony to a perturbation, the direct effect of the perturbation will be proportional to the abundance of the perturbed species, thus a value of α close to 2 (Lande *et al.*, 2003). We call this type of perturbation *environmental* as fluctuations of environmental variables typically affect all individuals of a given species, leading, e.g. to changes in the population growth rate (May, 1973b).

If individuals respond incoherently, e.g., some negatively and some positively, the direct effect of the perturbation will scale sublinearly with species abundance. For instance, demographic stochasticity can be seen as a perturbation resulting from the inherent stochasticity of birth and death events, which are typically assumed independent between individuals. In this case $\alpha = 1$, and we thus call such type *demographic* (Lande *et al.*, 2003).

We can also consider purely exogenous perturbations, such as the random removal or addition of individuals. In this case $\alpha = 0$. We call such perturbations *immigration*-type but stress that actual immigration events do not necessarily satisfy this condition (e.g., they can be density-dependent). Furthermore, because we focus on zero-mean perturbations, perturbations of this type contain as much *emigration* than immigration. The reasoning behind this nomenclature is that, in an open system, fluctuations of an otherwise constant influx of individuals would correspond to an immigration-type perturbation.

More generally, eq. (1) with $\alpha \in [0, 2]$ describes a continuum of perturbation types. Although not unrelated, the statistical relationship that defines perturbation type is not equivalent to Taylor's law (Taylor, 1961). The latter is an empirically observed power-law relationship between the variance and mean of population fluctuations. In contrast to the perturbation type α, the exponent of Taylor's law depends on community dynamics, e.g., on species interactions (Kilpatrick & Ives, 2003). We will come back to this point below and in the Discussion.

Perturbation intensity

For a given community, a stronger perturbation will lead to stronger fluctuations. A disproportionate increase in their amplitude as perturbation intensity changes would reveal nonlinearity in the dynamics (Zelnik *et al.*, 2019). In a linear setting, however, there is only a linear dependency on perturbation intensity. This trivial dependency can be removed by controlling for perturbation intensity. We now illustrate how to do so, for a given definition of variability.

Fluctuations induced by white-noise forcing are normally distributed, thus fully characterized by their variance and covariance. We thus construct a measure of variability based on the variance of species time-series. To compare variability of communities of different species richness we consider the average variance:

$$\sigma^2_{\text{out}} = \frac{1}{S}\sum_i \text{Var}(N_i(t)). \tag{2}$$

We now remove the trivial effect of perturbation intensity from eq. (2), starting from the one-dimensional system $dx/dt = -\lambda x + \sigma\xi(t)$. Its stationary variance is $\sigma^2_{\text{out}} = \frac{\sigma^2}{2\lambda}$. Here we see the combined effect of perturbation σ^2 and dynamics λ, leading us to define σ^2 as measure of perturbation intensity. For species-rich communities, we define perturbation intensity as the average intensity per species, that is, using the species-specific intensities σ_i^2:

$$\sigma^2_{\text{in}} = \frac{1}{S}\sum_i \sigma_i^2. \tag{3}$$

When increasing all species-specific perturbation intensities by a factor c, both σ^2_{in} and σ^2_{out} increase by the same factor. To remove this linear dependence, we define variability as

$$\mathcal{V} = \frac{\sigma^2_{\text{out}}}{\sigma^2_{\text{in}}}, \tag{4}$$

i.e., as the average species variance relative to perturbation intensity (see Ives *et al.*, 2003 for a similar definition). Generalizing previous work (Arnoldi *et al.*, 2016; Arnoldi & Haegeman, 2016) to all perturbation types, we construct *invariability* as

$$\mathcal{I} = \frac{1}{2\mathcal{V}}. \tag{5}$$

The factor $1/2$ allows $\mathcal{I}$ to coincide, for simple systems, with asymptotic resilience (Arnoldi *et al.*, 2016). In particular, for the one-dimensional example considered above for which $\mathcal{R}_\infty = \lambda$, we do have $\mathcal{V} = 1/2\lambda$ and thus $\mathcal{I} = \lambda = \mathcal{R}_\infty$.

Perturbation direction

At fixed intensity, perturbations can still differ in how their intensity is distributed and temporally correlated across species. Species with similar physiological traits will be affected in similar ways by, say, temperature fluctuations, whereas individuals from dissimilar species may react in unrelated, or even opposite, ways (Ripa & Ives, 2003). We thus study the effect of the covariance structure of the perturbation terms, i.e., the effect of the *direction* of perturbations. Spanning the set of all perturbation directions defines a whole range of community responses. Assuming some probability distribution leads to a probability distribution over the set of responses, i.e., a variability distribution (see Fig. 2). Finally, spanning the set of perturbation types reveals a continuous *family* of variability distributions. In Fig. 2 we show three archetypal elements of this family, corresponding to $\alpha = 0$ (blue distribution), $\alpha = 1$ (green distribution) and $\alpha = 2$ (red distribution).

For each distribution we consider two complementary statistics: mean- and worst-case responses. In Appendices 3 and 4 we prove that the worst-case response is always achieved by a perfectly coherent perturbation, i.e., a perturbation whose direct effects on species are not

independent, but on the contrary, perfectly correlated in time. We derive explicit formulas to compute the worst-case variability from the community matrix and species equilibrium abundances, see eqs. (C2, D5). The mean-case scenario, on the other hand, is defined with respect to a prior over the set of perturbation directions. For the least informative prior, we prove in Appendices 3 and 4 that a perturbation affecting all species independently but with equal intensity, realizes the mean-case response. This provides a way to compute this response from the community matrix and the species abundances, given in eqs. (C3, D6).

Results

Variability patterns for two-species community

We illustrate our variability framework on the following elementary example, in the form of a 2×2 community matrix

$$A = \begin{pmatrix} -1 & 0.1 \\ -4 & -1 \end{pmatrix}. \tag{6}$$

This matrix defines a linear dynamical system that could represent a predator-prey community, with the first species benefiting from the second at the latter's expense. Its asymptotic resilience is $\mathcal{R}_\infty = 1$. Let us suppose that the prey, N_2 (second row/column of A) is 7.5 times more abundant than its predator, N_1 (first row/column of A) and consider stochastic perturbations of this community, as formalized in eq. (1).

In Fig. 3 we represent the set of perturbation directions as a disc, in which every point is a unique perturbation direction (see Appendix 5 for details). The effect of a perturbation on a community is represented as a color; darker tones imply larger responses, with the baseline color (blue, green or red) recalling the perturbation type ($\alpha = 0, 1, 2$, respectively). Points

189 at the boundary of the disc correspond to coherent perturbations, which have the potential
190 to generate the largest (but also the smallest) variability. This is why the color maps of
191 Fig. 3 take their extreme values at the boundary. We see that variability strongly depends on
192 the perturbation direction, and that this dependence is strongly affected by the perturbation
193 type. For immigration-type perturbations (in blue) variability is largest when perturbing the
194 predator species most strongly (the least abundant species in this example). For demographic-
195 type perturbations (in green) perturbations that equally affect the two species but in opposite
196 ways achieve the largest variability. For environmental-type perturbations (in red) variability
197 is largest when perturbing the prey species (the most abundant species in this example). For
198 all types we see that positive correlations between the components of the perturbation (i.e.,
199 moving upwards on the disc) reduce variability (see Ripa & Ives, 2003 for related results).

200 Thus, in general, a given community cannot be associated to a single value of variability.
201 Depending on the type of perturbations causing variability, different species can have com-
202 pletely different contributions. This stands in sharp contrast with asymptotic resilience $\mathcal{R}_\infty$,
203 which associates a single stability value to the community. Although we know from previous
204 work (Arnoldi *et al.*, 2016) that the smallest invariability value in response to immigration-
205 type perturbations will always be smaller than $\mathcal{R}_\infty$, in general (i.e., any perturbation type
206 and/or any perturbation direction) there is, a priori, no reason to expect a relationship be-
207 tween invariability and asymptotic resilience.

208 Variability patterns in complex communities

209 The dimensionality of variability will be larger in communities comprised of many species,
210 as their sheer number, S, increases the dimension of the perturbation set quadratically. Yet,
211 when species interact, a generic structure can emerge from ecological assembly, revealing a

simple relationship between variability and the abundance of perturbed species. To show this, we study randomly assembled communities. We start from a large random pool of species and let the system settle to an equilibrium following Lotka-Volterra dynamics. During assembly species would go extinct, but no limit cycles, chaotic behavior or multi-stability were observed. A complete description of the nonlinear model is given in Appendix 6 and Matlab simulation code is available as supplementary material.

In Fig. 4 we show the variability patterns for a single randomly assembled community, but the results hold more generally (see below). The species pool consists of $S_{\text{pool}} = 50$ species, with species interaction strengths one order of magnitude weaker than species self-regulation. 40 species coexist in the community. In this species-rich context, the perturbation set cannot be represented exhaustively. We therefore plot the variability induced by species-specific perturbations (of various types) against the abundance of perturbed species. That is, we focus on the effect of a specific subset of perturbations, those affecting a single species. Linear combinations of these perturbations will span all scenarios in which species are affected independently, but exclude scenarios in which they are perturbed in systematically correlated or anti-correlated way.

The leftmost panel shows a negative unit slope on log scales: when caused by immigration-type perturbations, variability is inversely proportional to the abundance of perturbed species. Randomly adding and removing individuals from common species generates less variability than when the species is rare. In fact, the worst-case scenario corresponds to perturbing the rarest species. Worst-case invariability is close to asymptotic resilience, which corroborates previous findings showing that the long-term rate of return to equilibrium is often associated to rare species (Haegeman *et al.*, 2016; Arnoldi *et al.*, 2018). On the other hand, the middle panel of Fig. 4 shows that, in response to demographic-type perturbations, variability is independent of perturbed species' abundance. Finally, the rightmost panel shows a positive unit

slope on log scales: when caused by environmental-type perturbations, variability is proportional to the abundance of perturbed species. The worst case is thus attained by perturbing the most abundant one. Despite being more stable than rare ones (they buffer exogenous perturbations more efficiently, see left-hand panel), common species are more strongly affected by environmental perturbations, and can thus generate the most variability.

Those patterns are not coincidental, but emerge from species interactions, as we illustrate in Fig. 5. In their absence, other patterns can be envisioned. Without interactions, the response to a species-specific perturbation involves the perturbed species only. The variability-abundance relationship is then $\mathcal{V} = N^{\alpha}/2r$, with $N = K$. If r and K are statistically independent in the community (top-left panel in Fig. 5), this yields a different scaling than the one seen in Fig. 4. In the case of an r-K trade-off (i.e., species with larger carrying capacities have slower growth rate), abundant species would be the least stable species (bottom-left panel in Fig. 5, in blue) which is the opposite of what the leftmost panel of Fig. 4 shows. However, as interaction strength increases (from left to right in Fig. 5; the ratios of inter- to intraspecific interaction strength are 0, 0.02 and 0.1 approximately), we see emerging the relationship between abundance and variability of Fig. 4, regardless of the choice made for species growth rates and carrying capacities. We explain in Appendix 7 why this reflects a generic, limit-case behavior of complex communities. It occurs when species abundances, due to substantial indirect effects during assembly, become only faintly determined by their carrying capacities. This example demonstrates that this limit can be reached even for relatively weak interactions (in Fig. 4 and in the right-hand panels of Fig. 5, the interspecific interaction strengths are ten times smaller than the intraspecific ones).

Although we considered a specific section of the perturbation set, the response to single-species perturbations of immigration and environmental types can still span the whole variability distribution, from worst-case (rarest and most abundant species perturbed, respectively)

to mean- and best-case scenarios (most abundant and rarest species perturbed, respectively). For demographic-type perturbation the situation is more subtle as the response is independent of species abundance, and, in general, extreme scenarios will be associated to temporally correlated perturbations affecting multiple species.

The variability-abundance patterns shown in Figs. 4 and 5 should not be confused with Taylor's law (Taylor, 1961), a power-law relationship between a species' variance and its mean abundance. In fact, the variability-abundance pattern is *dual* to Taylor's law, it represents the community response to single-species perturbations instead of that of individual species to a community-wide perturbation.

Diversity-invariability relationships

To illustrate implications of the generic variability-abundance pattern, we revisit the diversity-stability relationship, with stability quantified as invariability $\mathcal{I}$. We assembled communities of increasing species richness S, each associated with an invariability distribution generated from random perturbations, predictions for mean- and worst-case scenarios, and a value of asymptotic resilience $\mathcal{R}_\infty$.

The leftmost panel of Fig. 6 shows a negative relationship between immigration-type invariability and species richness. Asymptotic resilience and worst-case invariability mostly coincide, with a decreasing rate roughly twice as large as that of the mean case. The middle panel suggests a different story. Mean-case demographic-type invariability stays more or less constant whereas the worst case diminishes with species richness, although much more slowly than $\mathcal{R}_\infty$. The relationship between diversity and stability is thus ambiguous. In the rightmost panel we see an increase in all realized environmental-type invariability values with species richness, showcasing a positive diversity-stability relationship.

The diversity stability relationships can be explained by the generic variability-abundance patterns of Figs. 4 and 5 (see Appendix 8). In the case of immigration-type perturbations, species contributions to variability are proportional to the inverse of their abundance (first panel of Fig. 4). The worst-case scenario follows the abundance of the rarest species, which rapidly declines with species richness. As detailed in Appendix 8, mean-case invariability scales as the average species abundance, which also typically decreases with S.

The responses to demographic perturbations, on the other hand, are not determined by any specific species abundance class (second panel of Fig. 4), so that no simple expectations based on typical trends of abundance distributions can be deduced.

We recover a simpler behavior when looking at the response to environmental-type perturbation: abundant species now drive variability (rightmost panel of Fig. 4). As explained in Appendix 8, mean-case invariability now scales as the *inverse* of an average species abundance. The latter typically declines with S explaining the observed increase of mean-case invariability.

There is an analogy to be made between stability and diversity. As has been said about diversity metrics (e.g., species richness, Simpson index or Shannon entropy), different invariability measures *"differ in their propensity to include or to exclude the relatively rarer species"* (Hill, 1973). In this sense, different invariability measures can probe different dynamical aspects of a same community, with potentially opposite dependencies on a given ecological parameter of interest.

Discussion

Because it is empirically accessible using simple time-series statistics, temporal variability is an attractive facet of ecological stability. But there are many ways to define variability

in models and empirical data, a proliferation of definitions reminiscent of the proliferation of definitions of stability itself (Grimm & Wissel, 1997). Variability measurements often depend, not only on the system of interest, but also on external factors that act as disturbances, which makes it difficult to relate variability to other stability concepts. These caveats constitute important obstacles toward a synthetic understanding of ecological stability, and its potential drivers (Ives & Carpenter, 2007).

We proposed to consider variability as a way to probe and measure an ecosystem's response to perturbations, thus revealing inherent dynamical properties of the perturbed system. We did not seek for an optimal, single measure of variability but, on the contrary, we accounted for a vast set of perturbations, leading to a whole distribution of responses. We focused on the worst- and mean-case values of this distribution as functions of species abundance, their interactions, and the *type* of perturbations that generates variability.

A perturbation type characterizes a statistical relationship between its direct effect on a population and the latter's abundance. We distinguished between environmental perturbations, whose direct effects on populations scales proportionally to their abundance; demographic perturbations, whose direct effect on populations scales sublinearly to their abundance; and purely exogenous perturbations, representing random addition and removal of individual, independent of the size of the perturbed population (immigration-type). Controlling for perturbation type and intensity, we considered all the ways this intensity can be distributed and correlated across species.

After having described a general (linear) theory for variability, which emphasizes its highly multidimensional nature, we turned our attention towards species-rich communities assembled by random (nonlinear) Lotka-Volterra dynamics. Because of the sheer number of species contained in such communities ($S \approx 40$ in our examples), we could have expected the dimensionality of perturbations and responses to be so large that variability distributions would be

too complex and broad to be clearly described. However, the process of assembly allowed for a simple behavior to emerge: a generic relationship between variability and the abundance of individually perturbed species. In essence, this pattern predicts that the species' ability to buffer exogenous perturbations is proportional to their abundance. In conjunction to this simple pattern, the type of perturbation will then determine the individual contributions of species to the variability distribution, so that both common and rare species can determine variability. This is reminiscent of diversity measures (Hill, 1973), some of which (e.g., species richness) are sensitive to the presence of rare species, while others are mostly indicative of the distribution of abundant species (e.g., Simpson diversity index).

These connections with different diversity metrics can explain contrasting trends in invariability as a function of species richness. Since immigration-type perturbations mostly affect rare species, they lead to a negative diversity-invariability relationship, reflecting a growing number and rarity of rare species. On the other hand, in response to demographic perturbations, species contributions to variability can be independent of their abundance. In this case, variability is not expected to follow trends in diversity, so that diversity-invariability patterns can be less predictable and harder to interpret. Finally, although common species buffer exogenous perturbations efficiently, they are also the most affected by environmental-type perturbations. This can lead to a proportional relationship between average abundance and mean-case invariability, and hence to a positive diversity-invariability relationship.

Implications for empirical patterns

We showed that species abundances greatly affect variability distributions. This new insight has broad consequences. For example, it has been reported that ecosystem-level and population-level stability tend to increase and decrease, respectively, with increasing diversity

(Jiang & Pu, 2009; Campbell *et al.*, 2011). Ecosystem-level stability is often quantified based on the variability of total biomass, which gives, by construction, a predominant weight to abundant species. On the other hand, averages of single-species variabilities have been used to measure population-level stability (Tilman, 1996). These averages are strongly affected, and can even be fully determined, by rare, highly variable species (Haegeman *et al.*, 2016). Thus, here as well as in our theoretical results (Fig. 6), stability metrics governed by common, or rare, species tend to generate respectively positive and negative diversity-stability relationships. It would be interesting to test whether this observation holds more generally, e.g., if it can explain the contrasting relationships recently reported by Pennekamp *et al.* (2018).

The type of perturbations affects which species abundance class contributes most to variability. In turn, the physical size of the system considered affects which perturbation type dominates. This is well known in population dynamics (Engen *et al.*, 2008), but it also transposes to the community level. At small spatial scales, implying small populations, we may expect variability to be driven by demographic stochasticity. At larger scales, implying larger populations, demographic stochasticity will be negligible compared with environmental perturbations. Just as changing the perturbation type transforms the respective roles of common and rare species, patterns of variability at different scales should reflect different aspects of a community (Chalcraft, 2013), associated to different species abundance classes (abundant species at large spatial scales, rare/rarer species at small spatial scales).

Empirically determining the perturbation type is a non-trivial task. To develop suitable methods, it might be helpful to first understand the link between the variability-abundance patterns (see Figs. 4 and 5) and Taylor's law (Taylor, 1961). The latter is an empirically accessible pattern, relating the mean and variance of population sizes. We studied the behavior of the community response to an individual species perturbation, while Taylor's law focuses on the individual species response to a perturbation of the whole community. This duality

also suggests that Taylor's law is, at the community level, strongly affected by species interactions. This is known (Kilpatrick & Ives, 2003), yet our approach could shed new light on the information regarding species interactions and other dynamical traits, actually contained in community-level Taylor's laws.

On the dimensionality of stability

We noted a connection between variability and asymptotic resilience, the most popular notion in theoretical studies (Donohue *et al.*, 2016). We showed that asymptotic resilience is comparable to the largest variability in response to an immigration-type perturbation, which is often a perturbation of the rarest species (first panel of Fig. 4). While asymptotic resilience is sometimes considered as a measure representative of collective recovery dynamics, we previously explained why that this is seldom the case (Arnoldi *et al.*, 2018). The asymptotic rate of return to equilibrium generally reflects properties of rare "satellite" species, pushed at the edge of local extinction by abundant "core" species. On the other hand, short-time return rates can exhibit qualitatively different properties related to more abundant species.

The multiple dimensions of variability are related to the multiple dimensions of return times. Variability is an integral measure of the transient regime following pulse perturbations, i.e., a superposition of responses to various pulses, some of which have just occurred and are thus hardly absorbed, while others occurred long ago and are largely resorbed. If abundant species are faster than rare ones (the case in complex communities, see Appendix 7), if they are also more strongly perturbed (e.g., by environmental perturbations), the bulk of the transient regime will be short: variability in response to environmental perturbations is associated with a short-term recovery. By contrast, if all species are, on average, equally displaced by perturbations (e.g., by immigration-type perturbations), rare species initially contribute to

the overall community displacement as much as do abundant ones. Since their recovery is typically very slow, the transient regime will be long: variability in response to immigration-type perturbations is associated with a long-term recovery.

Ecologists have long acknowledged the multi-faceted nature of ecological stability (Pimm, 1984; Grimm & Wissel, 1997; Ives & Carpenter, 2007; Donohue *et al.*, 2016), but here we show that a single facet (variability) is in itself inherently multidimensional, thus suggesting that links across facets can be subtle. Short-term return rates may be linked with environmental variability, but environmental variability may have nothing to do with immigration-type variability, the latter possibly related with long-term return rates and driven by rare species. Because measures can be determined by different species abundance classes, we should not expect a general and simple connection to hold between facets of ecological stability.

Conclusion

The multidimensional nature of variability can lead to conflicting predictions, but once this multidimensionality is acknowledged, it can be used to extensively probe the dynamical properties of a community. In particular, in species-rich systems, we revealed a generic pattern emerging from ecological assembly, relating species abundance to their variability contribution. This allowed connections to be drawn between variability and statistics of abundance distributions. We argued that similar patterns should underlie ecosystem responses to other families of perturbations (e.g., pulse perturbations). Therefore, we conclude that embracing the whole set of a ecosystem responses can help provide a unifying view on ecological stability and shed new light on the meaning of empirical and theoretical stability patterns.

Acknowledgements

We thank Matthieu Barbier, Nuria Galiana and Yuval Zelnik for helpful discussions and review of previous versions of this manuscript. Our work has benefited greatly from the thorough and constructive reviews of Frédéric Barraquand, Kévin Cazelles, Kevin McCann, and an anonymous reviewer. This work was supported by the TULIP Laboratory of Excellence (ANR-10-LABX-41) and by the BIOSTASES Advanced Grant, funded by the European Research Council under the European Union's Horizon 2020 research and innovation programme (grant agreement No 666971). This preprint has been reviewed and recommended by PCI Ecology (`https://dx.doi.org/10.24072/pci.ecology.100017`).

Literature Cited

Arnold, L. (1974). *Stochastic Differential Equations: Theory and Applications*. Dover Publications.

Arnoldi, J.F., Bideault, A., Loreau, M. & Haegeman, B. (2018). How ecosystems recover from pulse perturbations: A theory of short- to long-term responses. *Journal of Theoretical Biology*, 436, 79–92.

Arnoldi, J.F. & Haegeman, B. (2016). Unifying dynamical and structural stability of equilibria. *Proceedings of the Royal Society of London A: Mathematical, Physical and Engineering Sciences*, 472, 20150874.

Arnoldi, J.F., Loreau, M. & Haegeman, B. (2016). Resilience, reactivity and variability: A mathematical comparison of ecological stability measures. *Journal of Theoretical Biology*, 389, 47–59.

Campbell, V., Murphy, G. & Romanuk, T.N. (2011). Experimental design and the outcome and interpretation of diversity-stability relations. *Oikos*, 120, 399–408.

Chalcraft, D.R. (2013). Changes in ecological stability across realistic biodiversity gradients depend on spatial scale. *Global Ecology and Biogeography*, 22, 19–28.

Donohue, I., Hillebrand, H., Montoya, J.M., Petchey, O.L., Pimm, S.L., Fowler, M.S., Healy, K., Jackson, A.L., Lurgi, M., McClean, D., O'Connor, N.E., O'Gorman, E.J. & Yang, Q. (2016). Navigating the complexity of ecological stability. *Ecology Letters*, 19, 1172–1185.

Elton, C. (1946). Competition and the structure of ecological communities. *Journal of Animal Ecology*, 15, 54–68.

Engen, S., Lande, R. & Saether, B.E. (2008). A general model for analysing Taylor's spatial scaling laws. *Ecology*, 89, 2612–2622.

Fowler, M.S. & Ruokolainen, L. (2013). Colonization, covariance and colour: Environmental and ecological drivers of diversity–stability relationships. *Journal of theoretical biology*, 324, 32–41.

Griffin, J.N., O'Gorman, E.J., Emmerson, M.C., Jenkins, S.R., Klein, A.M., Loreau, M. & Symstad, A. (2009). *Biodiversity and the stability of ecosystem functioning*. Oxford University Press.

Grimm, V. & Wissel, C. (1997). Babel, or the ecological stability discussions: An inventory and analysis of terminology and a guide for avoiding confusion. *Oecologia*, 109, 323–334.

Gross, K., Cardinale, B.J., Fox, J.W., Gonzalez, A., Loreau, M., Wayne Polley, H., Reich, P.B. & van Ruijven, J. (2014). Species richness and the temporal stability of biomass production: A new analysis of recent biodiversity experiments. *The American Naturalist*, 183, 1–12.

Gurney, W. & Nisbet, R.M. (1998). *Ecological Dynamics*. Oxford University Press.

Haegeman, B., Arnoldi, J.F., Wang, S., de Mazancourt, C., Montoya, J.M. & Loreau, M. (2016). Resilience, invariability, and ecological stability across levels of organization. *bioRxiv*, 085852.

Hector, A., Hautier, Y., Saner, P., Wacker, L., Bagchi, R., Joshi, J., Scherer-Lorenzen, M., Spehn, E.M., Bazeley-White, E., Weilenmann, M., Caldeira, M.C., Dimitrakopoulos, P.G., Finn, J.A., Huss-Danell, K., Jumpponen, A., Mulder, C.P.H., Palmborg, C., Pereira, J.S., Siamantziouras, A.S.D., Terry, A.C., Troumbis, A.Y., Schmid, B. & Loreau, M. (2010).

General stabilizing effects of plant diversity on grassland productivity through population asynchrony and overyielding. *Ecology*, 91, 2213–2220.

Hill, M.O. (1973). Diversity and evenness: A unifying notation and its consequences. *Ecology*, 54, 427–432.

Ives, A.R. & Carpenter, S.R. (2007). Stability and diversity of ecosystems. *Science*, 317, 58–62.

Ives, A.R., Dennis, B., Cottingham, K.L. & Carpenter, S.R. (2003). Estimating community stability and ecological interactions from time-series data. *Ecological Monographs*, 73, 301–330.

Jiang, L. & Pu, Z. (2009). Different effects of species diversity on temporal stability in single trophic and multitrophic communities. *The American Naturalist*, 174, 651–659.

Kilpatrick, A.M. & Ives, A.R. (2003). Species interactions can explain Taylor's power law for ecological time series. *Nature*, 422, 65–68.

Lande, R., Engen, S. & Saether, B.E. (2003). *Stochastic Population Dynamics in Ecology and Conservation*. Oxford University Press.

MacArthur, R. (1955). Fluctuations of animal populations and a measure of community stability. *Ecology*, 36, 533–536.

May, R.M. (1973a). *Stability and Complexity in Model Ecosystems*. Princeton University Press.

May, R.M. (1973b). Stability in randomly fluctuating versus deterministic environments. *The American Naturalist*, 107, 621–650.

McCann, K.S. (2000). The diversity-stability debate. *Nature*, 405, 228–233.

Pennekamp, F., Pontarp, M., Tabi, A., Altermatt, F., Alther, R., Choffat, Y., Fronhofer, E.A., Ganesanandamoorthy, P., Garnier, A., Griffiths, J.I., Greene, S., Horgan, K., Massie, T.M., Mächler, E., Palamara, G.M., Seymour, M. & Petchey, O.L. (2018). Biodiversity increases and decreases ecosystem stability. *Nature*, 563, 109–112.

Pimm, S.L. (1984). The complexity and stability of ecosystems. *Nature*, 307, 321–326.

Pimm, S.L. (1991). *The Balance of Nature? Ecological Issues in the Conservation of Species and Communities*. University of Chicago Press.

Ripa, J. & Ives, A.R. (2003). Food web dynamics in correlated and autocorrelated environments. *Theoretical Population Biology*, 64, 369–384.

Ruokolainen, L., Linden, A., Kaitala, V. & Fowler, M.S. (2009). Ecological and evolutionary dynamics under coloured environmental variation. *Trends in Ecology & Evolution*, 24, 555–563.

Scheffer, M., Bascompte, J., Brock, W.A., Brovkin, V., Carpenter, S.R., Dakos, V., Held, H., van Nes, E.H., Rietkerk, M. & Sugihara, G. (2009). Early-warning signals for critical transitions. *Nature*, 461, 53–59.

Taylor, L.R. (1961). Aggregation, variance and the mean. *Nature*, 189, 732–735.

Tilman, D. (1996). Biodiversity: Population versus ecosystem stability. *Ecology*, 77, 350–363.

Tilman, D., Reich, P.B. & Knops, J.M.H. (2006). Biodiversity and ecosystem stability in a decade-long grassland experiment. *Nature*, 441, 629–632.

518 Tilman, D., Wedin, D. & Knops, J. (1996). Productivity and sustainability influenced by
519 biodiversity in grassland ecosystems. *Nature*, 379, 718–720.

520 Turelli, M. (1977). Random environments and stochastic calculus. *Theoretical Population*
521 *Biology*, 12, 140–178.

522 Van Kampen, N.G. (1997). *Stochastic Processes in Physics and Chemistry*. Elsevier.

523 Vasseur, D.A. & Yodzis, P. (2004). The color of environmental noise. *Ecology*, 85, 1146–1152.

524 Wang, S. & Loreau, M. (2014). Ecosystem stability in space: α, β and γ variability. *Ecology*
525 *Letters*, 17, 891–901.

526 Wang, S., Loreau, M., Arnoldi, J.F., Fang, J., Rahman, K.A., Tao, S. & de Mazancourt, C.
527 (2017). An invariability-area relationship sheds new light on the spatial scaling of ecological
528 stability. *Nature Communications*, 8, 15211.

529 Zelnik, Y.R., Arnoldi, J.F. & Loreau, M. (2019). The three regimes of spatial recovery.
530 *Ecology*, 100, e02586.

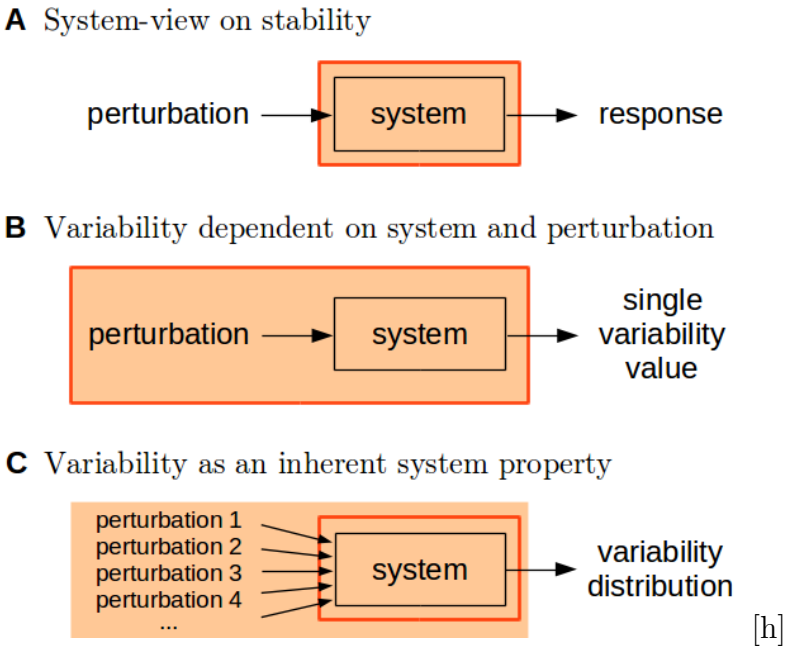

[h]

Figure 1: Variability vs stability. A: Stability quantifies the way a system responds to perturbations, seen as an inherent property of the system (indicated by the red framed box). B: By contrast, temporal variability is typically a feature of both the system studied and external factors that act as perturbations. C: For variability to be an inherent property of the system, one can consider a whole set of perturbations, thus integrating out the dependence on specific external factors.

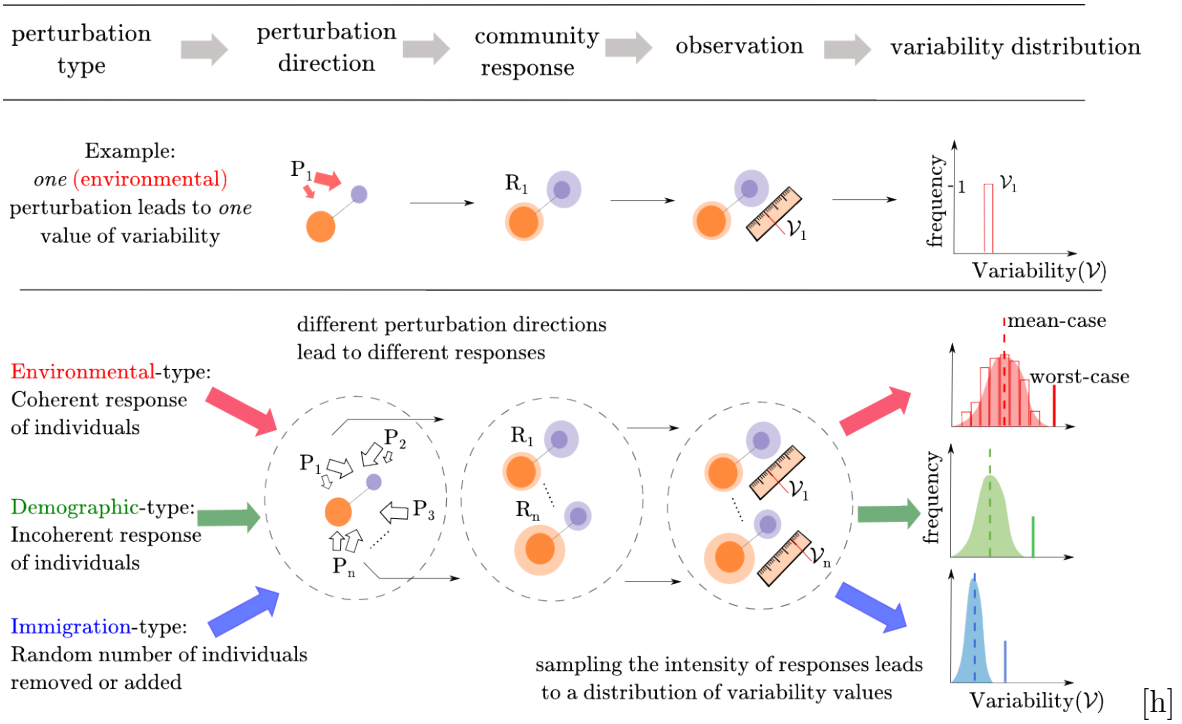

Figure 2: A theoretical framework for variability. Perturbations are characterized by their type, a statistical relationship between the direct effect of perturbations and the abundance of perturbed species. For a given type and fixed intensity, there remains a whole set of covariance structures of perturbations, i.e., various perturbation directions, that will be transformed by community dynamics into a whole set of community responses, i.e., various covariance structures of species stationary time series. A sampling of those responses leads to a variability distribution, one for each perturbation type. Spanning all perturbation types leads to a family of variability distributions (in blue, green and red in the rightmost column).

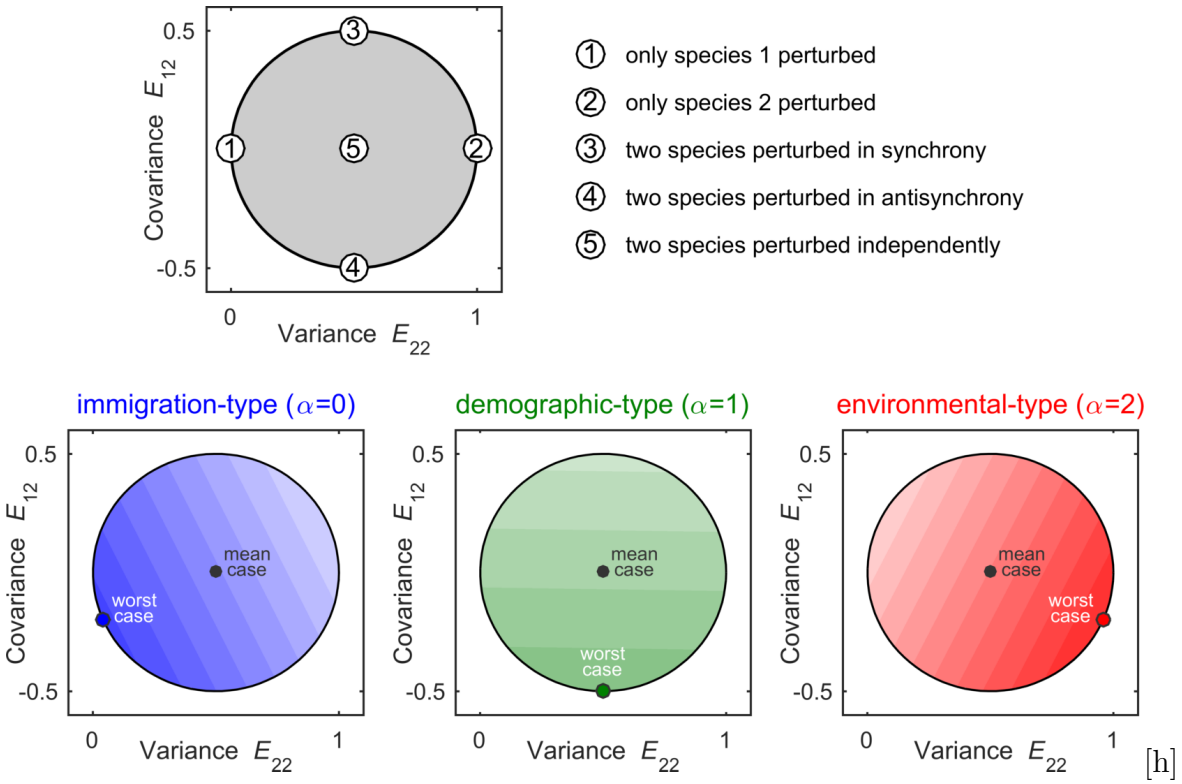

[h]

Figure 3: Variability patterns for a two-species community. Top panel: For a two-species community the set of all perturbation directions can be represented graphically as a disc (shaded in gray), with the variance of the perturbation term $\xi_2(t)$ on the x-axis and the covariance between $\xi_1(t)$ and $\xi_2(t)$ on the y-axis. Some special perturbation directions are indicated (numbers 1 to 5, see also Appendix 5). Bottom panels: We consider a predator-prey system; the community matrix A is given by eq. (6), and the prey (species 2) is 7.5 more abundant than its predator (species 1). The induced variability depends on the perturbation directions (darker colors indicate larger variability), and this dependence in turn depends on the perturbation type α. For immigration-type perturbations ($\alpha = 0$, in blue) variability is largest when perturbing species 1 most strongly. For demographic-type perturbations ($\alpha = 1$, in green) perturbations that affect the two species equally strongly but in opposite ways achieve the largest variability. For environmental-type perturbations ($\alpha = 2$, in red) variability is largest when perturbing species 2 most strongly. Notice that the worst case is always achieved by perturbations lying on the edge of the perturbation set. Such perturbations are perfectly correlated (see main text and Appendix 5).

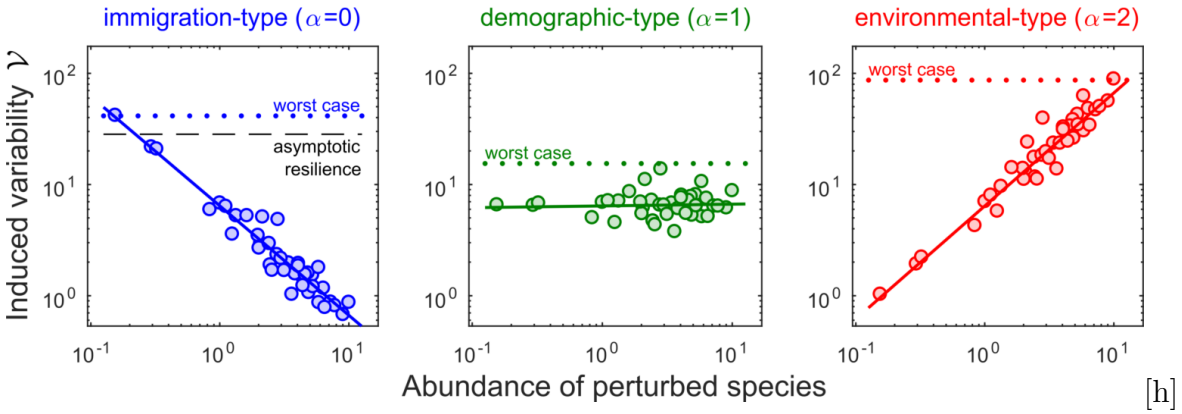

[h]

Figure 4: Variability-abundance pattern in a complex community. We consider a community of $S = 40$ species, and look at the variability induced by perturbing a single species, whose abundance is reported on the x-axis. Left: When caused by immigration-type perturbations ($\alpha = 0$), variability is inversely proportional to the abundance of the perturbed species (notice the log scales on both axis). The worst case is achieved by perturbing the rarest species, and is determined by asymptotic resilience (more precisely, it is close to $1/2\mathcal{R}_\infty$). Middle: For demographic-type perturbations ($\alpha = 1$), variability is independent of the abundance of the perturbed species. The worst case is not necessarily achieved by focusing the perturbation on one particular species. Right: For environmental-type perturbations ($\alpha = 2$), variability is directly proportional to the abundance of the perturbed species. The worst case is attained by perturbing the most abundant.

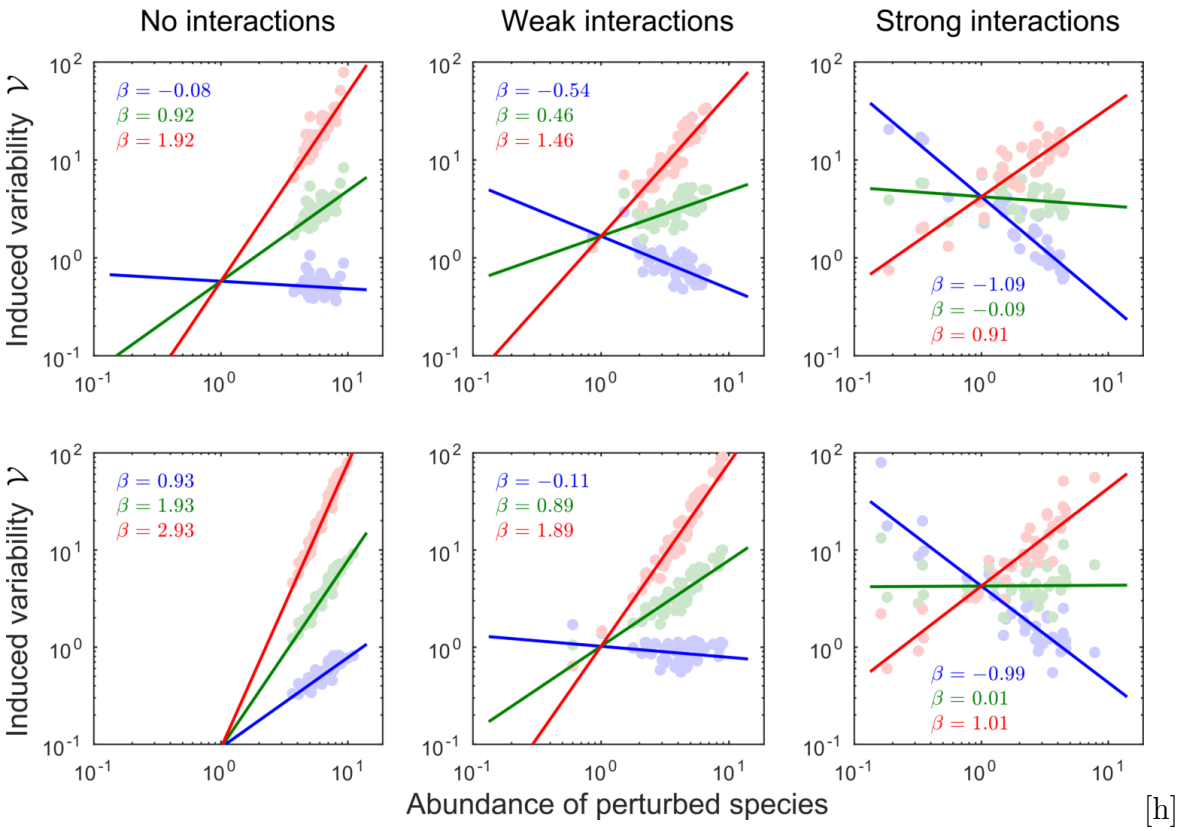

Figure 5: The emergence of the variability-abundance pattern (same procedure as in Fig. 4). Top row: intrinsic growth rates r and carrying capacities K are sampled independently. Bottom row: Species satisfy a r-K trade-off ($r \sim 1/K$). Colors correspond to the three perturbation types: $\alpha = 0$ (blue), $\alpha = 1$ (green) and $\alpha = 2$ (red). The value β reported in each panel corresponds to the exponent of the fitted relationship $V_i \propto N_i^{\beta}$ for each perturbation type. As interaction strength increases (left to right) we see emerging the relationship between abundance and variability described in Fig. 4, i.e., $\beta = \alpha - 1$. Thus when species interactions are sufficiently strong, variability always ends up being: (blue) inversely proportional, (green) independent and (red) directly proportional to the abundance of the perturbed species. Note that such relationships differ from Taylor's law: they represent an average community response to individual species perturbations, whereas Taylor's law deals with individual species responses to a perturbation of the whole community.

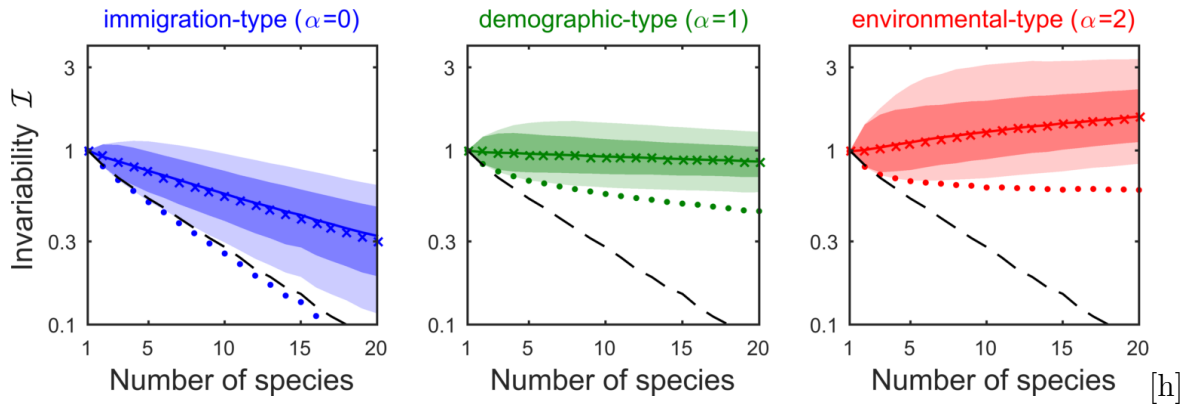

[h]

Figure 6: Different perturbation types yield contrasting diversity-stability relationships, with stability quantified as invariability $\mathcal{I}$. We generated random communities of increasing species richness S and computed their invariability distribution in response to 1000 random perturbations. Full line: median invariability, dark-shaded region: 5th to 95th percentile, light-shaded region: minimum to maximum realized values. The $\times$-marks correspond to the analytical approximation for the median, the dots to the analytical formula for the worst-case. Dashed line is asymptotic resilience $\mathcal{R}_\infty$. For immigration-type perturbations ($\alpha = 0$, blue) diversity begets instability, with $\mathcal{R}_\infty$ following worst-case invariability. For demographic-type perturbations ($\alpha = 1$, green) the trend is ambiguous. For environmental-type perturbations ($\alpha = 2$, red) all realized values of invariability increase with S.

Appendices to "The inherent multidimensionality of temporal variability: How common and rare species shape stability patterns"

Jean-François Arnoldi, Michel Loreau, and Bart Haegeman

The Appendices are organized as follows: Appendix A through D provides a self-contained presentation of the mathematical foundations of our variability theory. Appendix E through H provide details concerning specific applications considered in the main text: two-species communities in Appendix E, complex Lotka-Volterra communities in appendices F and G, and the link between abundance statistics and variability in Appendix H. A list of the most important notation used in the Appendices is given in Table A1.

1 Response to white-noise perturbation

We describe the response of a linear dynamical system, representing the dynamics of displacement of species around an equilibrium value, to a white-noise perturbation. Stochastic perturbations in continuous time are mathematically quite subtle (see, e.g., Turelli, 1977). However, in the setting of linear dynamical systems, the effect of a white-noise perturbation can be analyzed relatively easily. Because this analysis is not readily available in the ecology literature, we present here a short overview. We start from a fomulation in vector notation,

$$\frac{d\boldsymbol{x}}{dt} = A\boldsymbol{x} + \boldsymbol{\xi}(t), \tag{A1}$$

where $\boldsymbol{x} = (x_i)$ denotes the vector of species displacements, $\boldsymbol{\xi} = (\xi_i)$ the vector of species perturbations, and $A = (A_{ij})$ the community matrix.

Table A1: Notation used throughout the Appendices

symbol	meaning	equation
σ^2_{in}	per species variance of applied perturbation	(B2)
σ^2_{out}	per species variance of system response to perturbation	(B4, D3)
C_u	covariance matrix of individual pulses in multi-pulse perturbation	(A3)
f	frequency at which pulses occur in multi-pulse perturbation	
E	perturbation direction, proportional to fC_u	(B5)
C_x	covariance matrix of species responses to perturbation	(A5, A9)
$\mathcal{L}$	solution of Lyapunov equation, used to compute stationary C_x	(A7, A8)
$\mathcal{V}_\alpha$	variability for perturbation type α; when index α is omitted, immigration-type perturbations are assumed ($\alpha = 0$)	(D4)
$\mathcal{V}^{\text{worst}}$	mean-case variability, i.e., variability averaged over perturbation directions	(C2, D5)
$\mathcal{V}^{\text{mean}}$	worst-case variability, i.e., variability maximized over perturbation directions	(C3, D6)
$\mathcal{V}^{\text{spec } i}$	variability for the perturbation that affects only species i	
$\mathcal{I}$	invariability, i.e., variability-based stability measure	(B6)

Suppose that the perturbation $\boldsymbol{\xi}(t)$ consists in a sequence of pulses. We denote the times at which these pulses occur by t_k, and the corresponding pulse directions by $\boldsymbol{u}_k = (u_{k,i})$. The multi-pulse perturbation can then be written as

$$\boldsymbol{\xi}(t) = \sum_k \delta(t - t_k)\, \boldsymbol{u}_k. \tag{A2}$$

where we have used the Dirac delta function $\delta(t)$.

We model both the pulse times t_k and the pulse directions $\boldsymbol{u}_k$ as random variables. Specifically, we assume that the pulse times are distributed according to a Poisson point process with intensity f. This means that the probability that a pulse occurs in a small time interval of length Δs is equal to $f\Delta s$, and that this occurrence is independent of any other model randomness. We denote the average over the pulse times t_k by $\mathbb{E}_f$.

Furthermore, we assume that the pulse directions $\boldsymbol{u}_k$ are independent (mutually independent, and independent of any other model randomness) and identically distributed. They have zero mean, and their second moments are given by the covariance matrix C_u. That is, denoting the average over the pulse directions $\boldsymbol{u}_k$ by $\mathbb{E}_u$, we have $\mathbb{E}_u\, u_{k,i} = 0$, $\mathbb{E}_u\, u_{k,i}^2 = C_{u,ii}$, $\mathbb{E}_u\, u_{k,i}u_{k,j} = C_{u,ij}$, and $\mathbb{E}_u\, u_{k,i}u_{\ell,i} = \mathbb{E}_u\, u_{k,i}u_{\ell,j} = 0$ for $i \neq j$ and $k \neq \ell$. The latter equations can be written in vector notation,

$$C_u = \mathbb{E}_u\, \boldsymbol{u}_k \boldsymbol{u}_k^\top \qquad \text{and} \qquad \mathbb{E}_u\, \boldsymbol{u}_k \boldsymbol{u}_\ell^\top = 0. \tag{A3}$$

We use this information to compute the statistics of species displacements $\boldsymbol{x}(t)$. Because the system response to a single pulse perturbation at time t_k in directon $\boldsymbol{u}_k$ is equal to

$e^{(t-t_k)A}\boldsymbol{u}_k$, the system response to the sequence (A2) of pulse perturbations is equal to

$$\boldsymbol{x}(t) = \sum_{k|t_k<t} e^{(t-t_k)A}\,\boldsymbol{u}_k. \tag{A4}$$

Taking the mean over the perturbation directions, we obtain

$$\mathbb{E}_u\,\boldsymbol{x}(t) = \sum_{k|t_k<t} e^{(t-t_k)A}\,\mathbb{E}_u\,\boldsymbol{u}_k = 0,$$

showing that the species displacements fluctuate around the unperturbed equilibrium.

Next, we compute the covariance matrix of the species displacements,

$$C_x = \mathbb{E}_{f,u}\,\boldsymbol{x}(t)\boldsymbol{x}(t)^\top. \tag{A5}$$

We substitute the response to the multi-pulse perturbation, eq. (A4),

$$\begin{aligned}
C_x &= \mathbb{E}_{f,u} \sum_{k|t_k<t} e^{(t-t_k)A}\,\boldsymbol{u}_k \sum_{\ell|t_\ell<t} \boldsymbol{u}_\ell^\top\, e^{(t-t_\ell)A^\top} \\
&= \mathbb{E}_f \sum_{k|t_k<t} \sum_{\ell|t_\ell<t} e^{(t-t_k)A}\,\mathbb{E}_u\,\boldsymbol{u}_k\boldsymbol{u}_\ell^\top\, e^{(t-t_\ell)A^\top} \\
&= \mathbb{E}_f \sum_{k|t_k<t} e^{(t-t_k)A}\,\mathbb{E}_u\,\boldsymbol{u}_k\boldsymbol{u}_k^\top\, e^{(t-t_k)A^\top} \\
&= \mathbb{E}_f \sum_{k|t_k<t} e^{(t-t_k)A}\,C_u\,e^{(t-t_k)A^\top},
\end{aligned}$$

where we have used eq. (A3). To take the average over the pulse times, we partition the time

axis in small intervals of length Δs. Writing $s_n = n\Delta s$ for any integer n, we get

$$C_x = \sum_{n|s_n<t} e^{(t-s_n)A}\, C_u\, e^{(t-s_n)A^\top} f\Delta s,$$

because the contribution of term n is equal to $e^{(t-s_n)A}\, C_u\, e^{(t-s_n)A^\top}$ with probability $f\Delta s$, and zero otherwise. Assuming that the time intervals Δs are infinitesimal, we find the integral

$$\begin{aligned} C_x &= \int_{-\infty}^{t} e^{(t-s)A}\, C_u\, e^{(t-s)A^\top} f ds \\ &= \int_{0}^{\infty} e^{sA}\, C_u\, e^{sA^\top} f ds \\ &= \int_{0}^{\infty} e^{sA} \left(f C_u\right) e^{sA^\top} ds. \end{aligned} \tag{A6}$$

Hence, we have obtained the stationary covariance matrix of the species displacements under a stochastic multi-pulse perturbation.

A white-noise perturbation corresponds to a special case of the stochastic multi-pulse perturbation, namely, to the case of extremely frequent pulses (large f) of extremely small size (small $\|\boldsymbol{u}\|$). More precisely, we have to take the coupled limit $f \to \infty$ and $C_u \to 0$ while keeping fC_u constant. Because eq. (A6) depends on f and C_u through the product fC_u only, the same expression is also valid for white-noise perturbations.

Alternatively, the stationary covariance matrix C_x can be obtained by solving the so-called Lyapunov equation,

$$AC + CA^\top + E = 0, \tag{A7}$$

where E is the covariance matrix characterizing the white noise, equal to fC_u in our case.

Indeed, it can be verified that eq. (A6) satisfies eq. (A7),

$$\begin{aligned} AC_x + C_x A^\top &= \int_0^\infty \Big(A e^{sA}\, f C_u\, e^{sA^\top} ds + e^{sA}\, f C_u\, e^{sA^\top} A^\top \Big) ds \\ &= \int_0^\infty \frac{d}{ds} \Big(e^{sA}\, f C_u\, e^{sA^\top} \Big) ds \\ &= e^{sA}\, f C_u\, e^{sA^\top} \Big|_{s\to\infty} - e^{sA}\, f C_u\, e^{sA^\top} \Big|_{s=0} \\ &= -f C_u. \end{aligned}$$

For a stable matrix A this is the unique solution of the Lyapunov equation, for which we introduce the short-hand notation $\mathcal{L}(A, E)$,

$$\mathcal{L}(A, E) = \int_0^\infty e^{sA}\, E\, e^{sA^\top} ds. \tag{A8}$$

Hence, we can write

$$C_x = \mathcal{L}(A, f C_u), . \tag{A9}$$

From a numerical viewpoint, the covariance matrix C_x can be easily obtained by solving the Lyapunov eq. (A7), which can be written as a system of S^2 linear equations, rather than by computing the integral in (A8). Note also that solution of Lyapunov equation is linear in the perturbation covariance matrix,

$$\mathcal{L}(A, c_1 E_1 + c_2 E_2) = c_1\, \mathcal{L}(A, E_1) + c_2\, \mathcal{L}(A, E_2). \tag{A10}$$

2 Construction of variability measure

We explain the construction of the variability measure $\mathcal{V}$, see eq. (4) in the main text. The construction is based on the comparison of the intensity of the system response relative to the intensity of the applied perturbation. It should be stressed that, while we take special care of quantifying these intensities in a reasonable way, alternative choices are possible.

Perturbation intensity A reasonable measure of the perturbation intensity should increase with the number of pulses and the intensity of each pulse separately. In particular, we expect it to be proportional to the pulse frequency f and to some function of the pulse covariance matrix C_u.

We propose to look at the squared displacements $\|\boldsymbol{u}_k\|^2$ induced by pulses $\boldsymbol{u}_k$. The accumulated squared displacement in time interval $[t, t+T]$ is

$$\sum_{t_k \in [t,t+T]} \|\boldsymbol{u_k}\|^2.$$

Taking the average over pulse times and pulse directions,

$$\mathbb{E}_{f,u} \sum_{t_k \in [t,t+T]} \|\boldsymbol{u_k}\|^2 = \sum_{n | t < s_n < t+T} \mathbb{E}_u \|\boldsymbol{u}\|^2 \, f \Delta s,$$

where we have partitioned the time axis in small intervals of length Δs (see derivation of eq. (A6)). Then,

$$\mathbb{E}_{f,u} \sum_{t_k \in [t,t+T]} \|\boldsymbol{u_k}\|^2 = \mathrm{Tr}\big(C_u\big) fT.$$

The result is proportional to the length T of the considered time interval. The average

accumulated squared displacement per unit of time is

$$\frac{1}{T}\,\mathbb{E}_{f,u}\sum_{t_k\in[t,t+T]}\|\boldsymbol{u_k}\|^2=\mathrm{Tr}\big(fC_u\big). \tag{B1}$$

As expected, this quantity is proportional to the pulse frequency f and increases with the pulse covariance matrix C_u. Note also that f and C_u appear as a product, so that the expression is compatible with the white-noise limit.

Eq. (B1) quantifies the intensity of the perturbation applied to the entire ecosystem. This measure is not directly appropriate to normalize the pertubation intensity across systems. Indeed, when keeping the total perturbation intensity constant, the perturbation applied to a given species would be weaker in a community with a larger number of species. To eliminate this artefact, we normalize the perturbation intensity on a per species basis. Thus, we propose to quantify the perturbation intensity as

$$\sigma_{\mathrm{in}}^2=\frac{f}{S}\,\mathrm{Tr}\,C_u. \tag{B2}$$

Response intensity We measure the intensity of the system response in terms of the covariance matrix C_x. This matrix encodes the statistical properties of the abundance (or biomass) fluctuations in stationary state. For example, species abundance $x_i(t)$ fluctuates around its equilibrium value N_i with variance $C_{x,ii}$. More generally, we can describe the fluctuations of any function φ of species abundance. The dynamics near equilibrium are

$$\varphi(\boldsymbol{n}(t))=\varphi(\boldsymbol{N})+\boldsymbol{v}^\top\boldsymbol{x}(t),$$

where vector $\boldsymbol{v}=\nabla\varphi$ is the gradient of the function φ evaluated at the equilibrium $\boldsymbol{N}$. This vector gives the direction in which the system fluctuations are observed. Then, denoting the

temporal mean and variance by $\mathbb{E}_t$ and Var_t, we have

$$\begin{aligned}\mathrm{Var}_t\left(\varphi(\boldsymbol{n}(t)\right) &= \mathbb{E}_t\Big(\big(\boldsymbol{v}^\top \boldsymbol{x}(t)\big)^2\Big)\\ &= \mathbb{E}_t\Big(\boldsymbol{v}^\top \boldsymbol{x}(t)\boldsymbol{x}(t)^\top \boldsymbol{v}\Big)\\ &= \boldsymbol{v}^\top \mathbb{E}_t\big(\boldsymbol{x}(t)\boldsymbol{x}(t)^\top\big)\boldsymbol{v}\\ &= \boldsymbol{v}^\top C_x\, \boldsymbol{v}. \end{aligned} \tag{B3}$$

We use this variance to quantify the intensity of the system response. Rather than choosing a particular vector $\boldsymbol{v}$, we consider the average over all observation directions. Specifically, we restrict attention to unit vectors $\boldsymbol{v}$ and average over the uniform distribution of such vectors. Denoting this average by $\mathbb{E}_v$, we get

$$\mathbb{E}_v\, \mathrm{Var}_t\big(\varphi(\boldsymbol{n}(t)\big) = \mathbb{E}_v\left(\boldsymbol{v}^\top C_x \boldsymbol{v}\right) = \mathrm{Tr}\; \mathbb{E}_v\, \boldsymbol{v}\boldsymbol{v}^\top C_x.$$

It follows from species symmetry that the average $\mathbb{E}_v\, \boldsymbol{v}\boldsymbol{v}^\top$ is proportional to the unit matrix. Moreover, because $\mathrm{Tr}\; \boldsymbol{v}\boldsymbol{v}^\top = 1$ for all vectors $\boldsymbol{v}$, the constant of proportionality is equal to $\frac{1}{S}$. Hence,

$$\mathbb{E}_v\, \mathrm{Var}_t\big(\varphi(\boldsymbol{n}(t)\big) = \frac{1}{S}\mathrm{Tr}\, C_x.$$

Therefore, we propose to quantify the response intensity as

$$\sigma^2_{\mathrm{out}} = \frac{1}{S}\mathrm{Tr}\, C_x. \tag{B4}$$

Variability and invariability We define variability $\mathcal{V}$ as the ratio of the response intensity σ^2_{out} and the perturbation intensity σ^2_{in},

$$\mathcal{V} = \frac{\sigma^2_{\text{out}}}{\sigma^2_{\text{in}}} = \frac{\frac{1}{S}\operatorname{Tr} C_x}{\frac{f}{S}\operatorname{Tr} C_u} = \frac{\operatorname{Tr} C_x}{f \operatorname{Tr} C_u}.$$

Substituting eq. (A9) for C_x, we get

$$\mathcal{V} = \frac{\operatorname{Tr} \mathcal{L}(A, fC_u)}{f \operatorname{Tr} C_u} = \operatorname{Tr} \mathcal{L}\big(A, \frac{C_u}{\operatorname{Tr} C_u}\big),$$

where we have used the linearity property (A10). We see that only the normalized perturbation covariance matrix matters in this expression. That is, the variability measure focuses on the directional effect of the perturbation. We make this dependence explicit in the notation, and write

$$\mathcal{V}(E) = \operatorname{Tr} \mathcal{L}(A, E), \tag{B5}$$

where $E = \frac{C_u}{\operatorname{Tr} C_u}$ is the perturbation direction, i.e., a covariance matrix with unit trace.

Variability is inversely related to stability: the more variable an ecosytem, the less stable it is. For purpose of comparison, we construct a stability measure based on variability $\mathcal{V}(E)$, which we call invariability $\mathcal{I}(E)$,

$$\mathcal{I}(E) = \frac{1}{2\,\mathcal{V}(E)}. \tag{B6}$$

The factor 2 in this definition guarantees that we recover asymptotic resilience for the simplest dynamical systems. To see this, consider a system of S non-interacting species, in which all species have the same return rate λ. The community matrix is equal to $A = -\lambda \mathbb{1}$ where $\mathbb{1}$ denotes the identity matrix. From the Lyapunov equation (A7) we get the stationary covariance matrix $\mathcal{L}(A, E) = \frac{1}{2\lambda}E$. Therefore, $\mathcal{V}(E) = \frac{1}{2\lambda}$ and $\mathcal{I}(E) = \lambda$, which is equal to

the asymptotic resilience of this example system.

3 Worst-case and mean-case variability

Worst-case variability is defined as

$$\mathcal{V}^{\text{worst}} = \max_E \mathcal{V}(E) = \max_E \operatorname{Tr} \mathcal{L}(A, E) \tag{C1}$$

where the maximum is taken over perturbation directions, i.e., over covariance matrices E with $\operatorname{Tr} E = 1$. The function $\operatorname{Tr} \mathcal{L}(A, E)$ is linear in the perturbation direction E, see eq. (A10), and the set of perturbation directions is convex. Hence, the maximum is reached at an extreme point, that is, on the boundary of the set. The extreme points are the purely directional perturbations (see Appendix 5 for the argument in the two-species case), so that the maximum is reached at a purely directional perturbation. Arnoldi *et al.* (2016) showed that the worst-case variability can be easily computed, namely, as a specific norm of the operator $\widehat{A}^{-1}$ that maps E to $\mathcal{L}(A, E)$. Concretely, defining $\widehat{A} = A \otimes \mathbb{1} + \mathbb{1} \otimes A$,

$$\mathcal{V}^{\text{worst}} = ||\widehat{A}^{-1}||, \tag{C2}$$

where $|| \cdot ||$ stands for the spectral norm of $S^2 \times S^2$ matrices.

To define **mean-case variability** $\mathcal{V}^{\text{mean}}$, we assume a probability distribution over the perturbation directions, and compute the mean system response over this distribution. Due to the linearity property (A10), this mean response is equal to the response to the mean perturbation direction. Hence, we do not have to specify the full probability distribution over the perturbation directions; it suffices to determine the mean perturbation direction. As can be directly verified in the two-species case (Appendix 5), if, averaged over the distribution

of perturbation directions, perturbation intensities are evenly distributed across species, and positive and negative correlations between species perturbations cancel out, then the mean perturbation direction is adirectional. This corresponds to the center of the set of perturbation directions (in the two-species case the disc center represented in Fig. 3), and is proportional to the identity matrix, that is, $E = \frac{1}{S}\mathbb{1}$. Therefore,

$$\mathcal{V}^{\text{mean}} = \operatorname{Tr} \mathcal{L}(A, \tfrac{1}{S}\mathbb{1}). \tag{C3}$$

4 Perturbation types and variability

The perturbation type (environmental-, demographic- or immigration-type) affects how the perturbation intensity is distributed across species. Therefore, it also affects our measure of variability, as defined in Appendix 2. Here we describe how the variability definition has to be modified.

We defined variability measure (B5) as the intensity of the system response relative to the intensity of the applied perturbation. To quantify the perturbation intensity in the case of abundance-dependent perturbations, we distinguish the intrinsic effect of the perturbation on a species, which does not depend on the species' abundance, and the total effect of the perturbation on the species, which does depend on abundance. We propose to express the perturbation intensity in terms of the intrinsic perturbation, while it is the total perturbation that acts on the species dynamics.

Formally, for species i, we denote the intrinsic perturbation by $\xi_i^{\text{intr}}(t)$ and the total perturbation by $\xi_i^{\text{tot}}(t)$. Then, for a type-α perturbation, we have

$$\xi_i^{\text{tot}}(t) = N_i^{\frac{\alpha}{2}}\, \xi_i^{\text{intr}}(t), \tag{D1}$$

where N_i is the abundance of species i. Thus, the intrinsic perturbation $\xi^{\text{intr}}(t)$ can be interpreted as the per capita perturbation strength. Eq. (D1) can be written in vector notation as

$$\boldsymbol{\xi}^{\text{tot}}(t) = D^{\frac{\alpha}{2}}\boldsymbol{\xi}^{\text{intr}}(t), \tag{D2}$$

where D is the diagonal matrix whose entries are species equilibrium values ($D_{ii} = N_i$).

Both the intrinsic and total perturbation are multi-pulse. If we denote the pulses of the intrinsic perturbation by $\boldsymbol{u}_k$, then, by eq. (D2), those of the total perturbation are $D^{\frac{\alpha}{2}}\boldsymbol{u}_k$. Then, to quantify the perturbation intensity, we use the covariance matrix of the pulses in the intrinsic perturbation. The derivation leading to eq. (B2) is still valid. However, to compute the covariance matrix of the species displacements, we use the covariance matrix of the pulses in the total perturbation. This corresponds to replacing C_u by $D^{\frac{\alpha}{2}}C_uD^{\frac{\alpha}{2}}$ in the derivation of eq. (B4), so that we get

$$\sigma^2_{\text{out}} = \frac{1}{S}\text{Tr}\,\mathcal{L}\big(A, fD^{\frac{\alpha}{2}}C_uD^{\frac{\alpha}{2}}\big). \tag{D3}$$

The variability measure for a type-α perturbation becomes

$$\mathcal{V}_\alpha = \frac{\sigma^2_{\text{out}}}{\sigma^2_{\text{in}}} = \text{Tr}\,\mathcal{L}\big(A, \frac{D^{\frac{\alpha}{2}}C_uD^{\frac{\alpha}{2}}}{\text{Tr}\,C_u}\big),$$

or, in terms of the (intrinsic) perturbation direction E,

$$\mathcal{V}_\alpha(E) = \text{Tr}\,\mathcal{L}\big(A, D^{\frac{\alpha}{2}}ED^{\frac{\alpha}{2}}\big). \tag{D4}$$

Applying the same arguments as in Appendix 3, we find that worst-case variability,

$$\mathcal{V}^{\text{worst}}_\alpha = \max_E\ \mathcal{V}_\alpha(E) = \max_E\ \text{Tr}\,\mathcal{L}\big(A, D^{\frac{\alpha}{2}}ED^{\frac{\alpha}{2}}\big),$$

is attained at a perfectly correlated perturbation. If we define the operator (an $S^2 \times S^2$ matrix)

$$\mathcal{D}_\alpha = D^{\frac{\alpha}{2}} \otimes D^{\frac{\alpha}{2}},$$

then the worst case-variability can be computed as

$$\mathcal{V}_\alpha^{\text{worst}} = ||\widehat{A}^{-1} \circ \mathcal{D}_\alpha||, \tag{D5}$$

where $||\cdot||$ is the spectral norm for $S^2 \times S^2$ matrices. On the other hand, the mean-case variability,

$$\mathcal{V}_\alpha^{\text{mean}} = \operatorname{Tr} \mathcal{L}\big(A, \tfrac{1}{S} D^\alpha\big), \tag{D6}$$

is attained by the uniform, uncorrelated perturbation.

5 Perturbation directions in two dimensions

Variability spectra are built on the notion of perturbation directions. They are characterized by a covariance matrix E with $\operatorname{Tr} E = 1$. To gain some intuition, we study the set of perturbation directions in the case of two species.

Any perturbation direction E in two dimensions can be written as

$$E = \begin{pmatrix} 1-x & y \\ y & x \end{pmatrix}. \tag{E1}$$

with $0 \leq x \leq 1$ and $y^2 \leq x(1-x)$. The first inequality guarantees that the elements on the diagonal are variances, i.e., positive numbers. The second inequality guarantees that the off-diagonal element is a proper covariance, in particular, that the correlation coefficient is

contained between -1 and 1. Note that matrix (E1) has always $\mathrm{Tr}\, E = 1$.

It follows from eq. (E1) that the set of perturbation directions in two dimensions is parameterized by two numbers x and y. Using these numbers as axes of a two-dimensional plot, we see that the set of perturbation directions corresponds to a disc with radius 0.5 and centered at $(0.5, 0)$ (see Fig. 3).

It is instructive to study the position of specific perturbation directions on the disc. The point $(0, 0)$ corresponds to a perturbation affecting only the first species, whereas point $(1, 0)$ is a perturbation only affecting the second species. More generally, any point on the boundary of the disc correspond to a multi-pulse perturbation for which the individual pulses have a fixed direction. For example, the point $(0.5, 0.5)$ is a perturbation for which each pulse has the same effect on species 1 and species 2, whereas the perturbation corresponding to point $(0.5, -0.5)$ consists of pulses that affect the two species equally strongly, but in an opposite way. Perturbations on the boundary are *perfectly correlated*.

The perturbations towards the center of the disc are composed of pulses with more variable directions. For example, a multi-pulse perturbation for which half of the pulses affect only the second species, and the other pulses affect the two species equally strongly corresponds to the point $\frac{1}{2}(0, 1) + \frac{1}{2}(0.5, 0.5) = (0.25, 0.75)$. The mixture of different pulse directions is the strongest at the center of the disc $(0.5, 0)$. Examples of ways to realize this perturbation are $\frac{1}{2}(0, 0) + \frac{1}{2}(1, 0)$, $\frac{1}{2}(0.5, 0.5) + \frac{1}{2}(0.5, -0.5)$ and $\frac{1}{4}(0, 0) + \frac{1}{4}(0.5, 0.5) + \frac{1}{4}(1, 0) + \frac{1}{4}(0.5, -0.5)$. In each of these example, the pulses have their intensities, averaged over time, evenly distributed across species, and affect them, again averaged over time, in an uncorrelated way. The perturbation corresponding to the point $(0.5, 0)$ is thus evenly distributed across species but uncorrelated in time.

6 Random Lotka-Volterra model

The communities used in Figs. 4, 5 and 6 are constructed from the Lotka-Volterra model with random parameters. We consider a pool of species governed by the dynamics

$$\frac{dN_i(t)}{dt} = \frac{r_i N_i(t)}{K_i}\left(K_i - N_i - \sum_{\substack{j=1 \\ j\neq i}}^{S_{\text{pool}}} B_{ij}N_j(t)\right), \tag{F1}$$

and we let the dynamics settle to an equilibrium community of S remaining species. By drawing random values for the parameters – growth rates r_i, carrying capacities K_i, and competition coefficients B_{ij} – we generate communities of various diversity.

For the communities in Fig. 4, we set $S_{\text{pool}} = 50$, and chose the parameter values as follows,

- r_i randomly drawn from $\mathcal{N}(1, 0.2)$, a normal distribution with mean 1 and standard deviation 0.2 (independent draws for different species)
- K_i drawn from $\mathcal{N}(1, 0.2)$
- B_{ij} half of the competition coefficients are set equal to 0; the other half are drawn from $\mathcal{N}(0.1, 0.1)$.

This procedure resulted in a community of $S = 40$ persistent species. Note that some of the competition coefficients can be negative, so that there can be positive interactions (e.g. facilitation).

For the communities in the top row of Fig. 5, we followed the same procedure, except that we changed the way of generating the competition coefficients B_{ij}. In the case without interactions, all B_{ij} were set zero; in the case with weak interactions, the non-zero coefficients B_{ij} were drawn from $\mathcal{N}(0.02, 0.02)$; and in the case with strong interactions, the non-zero B_{ij} were drawn from $\mathcal{N}(0.1, 0.1)$, as for the community of Fig. 4.

We applied a similar procedure to obtain the bottom row of Fig. 5, but for these communities the growth rates r_i and carrying capacities K_i were not drawn independently. Instead, we first drew auxiliary variables a_i from $\mathcal{N}(1, 0.2)$, b_i from $\mathcal{N}(1, 0.1)$ and c_i from $\mathcal{N}(1, 0.1)$, and then set $r_i = b_i a_i$ and $K_i = c_i/a_i$.

For the communities of Fig. 6, we varied the size of the species pool S_{pool} so that the realized species richness covered the range from 1 to 20. Specifically, we drew S_{pool} randomly from 1 to 100, and generated the parameter values as in Fig. 4. We repeated this procedure many times, until obtaining 1000 communities for each value of realized species richness S from 1 to 20. Then, for each realized community, and for each of the three perturbation types ($\alpha = 0$, $\alpha = 1$ and $\alpha = 2$), we generated 1000 random perturbations leading to a variability distribution of 1000 values. From the variability distributions we extracted median, 5th and 95th percentile, and minimum and maximum. For the realized communities we computed asymptotic resilience, worst-case variability and the prediction for the median. Finally, we computed the median of these statistics and predictions, all represented in Fig. 6.

7 Genericity in strongly interacting communities

We give some elements as to why the behavior reported in Figs. 4 and 5 in the main text can be expected to be a general trend in diverse communities of interacting species. Denote by $\mathcal{V}_\alpha^{\text{spec } i}$ the community variability induced by a type-α perturbation that is fully focused on a single species i. We are interested in the relationship between this variability and the equilibrium abundance N_i of the perturbed species i.

First, note that for single-species perturbations the variability metrics $\mathcal{V}_\alpha^{\text{spec } i}$ for different

perturbation types α are directly linked. From definition (D4) we get that

$$\mathcal{V}_{\alpha}^{\text{spec } i} = N_i^{\alpha}\, \mathcal{V}_{\alpha=0}^{\text{spec } i}. \tag{G1}$$

Hence, it suffices to study the behavior of $\mathcal{V}_{\alpha=0}^{\text{spec } i}$.

Next, consider again the Lotka-Volterra dynamics (F1) from the perspective of a focal species i. If a stable equilibrium exists in which the focal species survives, small displacements from equilibrium $x_i = N_i(t) - N_i$ are met with the dynamics

$$\frac{dx_i}{dt} = \frac{r_i N_i}{K_i}\Big(- x_i - \sum_{j\neq i} B_{ij} x_j \Big) = \frac{1}{\tau_i}\Big(- x_i - \sum_{j\neq i} B_{ij} x_j \Big), \tag{G2}$$

where $\tau_i = \frac{K_i}{r_i N_i}$ has units of time. We claim that τ_i sets a characteristic time scale of the focal species dynamics; it measures the typical time it takes for the species to recover from a perturbation that displaces it from its equilibrium. This species response time is directly related to the species' variability $\mathcal{V}_{\alpha=0}^{\text{spec } i}$: the slower the species, the larger the impact of a repeated perturbation acting on this species, and the larger the induced variability.

We illustrate the relationship between τ_i and $\mathcal{V}_{\alpha=0}^{\text{spec } i}$ in Fig. G1 (inset panels). For the six communities of Fig. 5, we fit the power-law relationship

$$\mathcal{V}_{\alpha=0}^{\text{spec } i} \propto \tau_i^{\nu}, \tag{G3}$$

where the index i runs over the set of persistent species. The estimates of the exponent ν (using linear regression on the log-log plot) are all close to one. This result is obvious for the communities without interactions, for which $\mathcal{V}_{\alpha=0}^{\text{spec } i} = \frac{1}{2}\tau_i$ (left-hand panels). But the same result remains valid in the presence of interactions. We find that interactions do not substantially modify the time scale on which a species responds to perturbations affecting

only that species.

Therefore, to study the relationship between N_i and $\mathcal{V}_\alpha^{\text{spec } i}$, we can restrict to the simpler relationship between N_i and $\tau_i = \frac{K_i}{r_i N_i}$, which is determined by the correlations between growth rates r_i, carrying capacities K_i and equilibrium abundances N_i. Fig. G1 (main panels) shows this relationship for the six communities of Fig. 5. Fitting the power law

$$\tau_i \propto N_i^\gamma, \tag{G4}$$

we find various estimates for the exponent γ. Without interactions, we have $N_i = K_i$, and hence, $\tau_i = \frac{1}{r_i}$. If growth rates and carrying capacities are drawn independently, abundance and response time are unrelated, leading to $\gamma \approx 0$ (Fig. G1, upper-left panel). Alternatively, if growth rates and carrying capacities satisfy some trade-off, higher abundance (larger K_i) is associated with longer response time (smaller r_i), leading to $\gamma > 0$ (Fig. G1, lower-left panel). When increasing the interactions, the link between N_i and K_i becomes weaker. Indeed, from the equilibrium condition for species i we have

$$\begin{aligned} N_i &= K_i + \sum_{j\neq i} B_{ij} N_j \\ &= K_i + \Bigg(\sum_{j\neq i} B_{ij} K_j + \sum_{k\neq j\neq i} B_{ij} B_{jk} K_k \\ &+ \sum_{l\neq k\neq j\neq i} B_{ij} B_{jk} B_{kl} K_l + \dots \Bigg), \end{aligned}$$

where in the second line we have used the equilibrium condition for the other species. For sufficiently strong interactions, the terms between brackets dominate the term K_i, so that N_i and K_i become unrelated. In this case, we have $\tau_i \propto \frac{1}{N_i}$, leading to $\gamma \approx -1$: more abundant species have faster dynamics and smaller response time. This limiting case is observed both

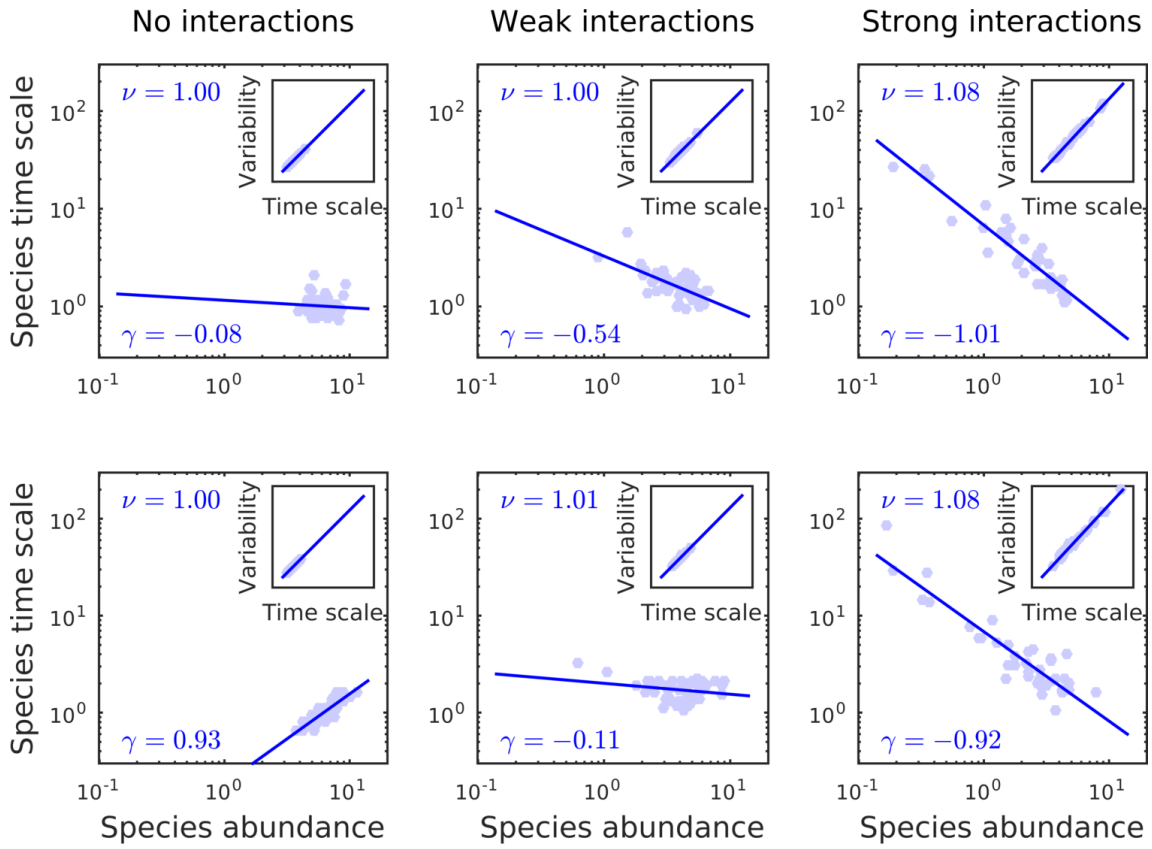

Figure G1: Clarifying the relationship between abundance of perturbed species and community variability. In Appendix 7 we introduce the auxiliary variable τ_i, the characteristic time scale of species i, to explain the relationship between variability $\mathcal{V}_{\alpha=0}^{\text{spec } i}$ and abundance N_i. For the six communities of Fig. 5 in the main text, we plot τ_i vs N_i in the main panels, and $\mathcal{V}_{\alpha=0}^{\text{spec } i}$ vs τ_i in the inset panels. We fit a power law to each of these relationships, using linear regression on the log-log plot. The estimated exponents γ (for the data τ_i vs N_i) and ν (for the data $\mathcal{V}_{\alpha=0}^{\text{spec } i}$ vs τ_i) are reported in the panels.

if r_i and K_i are independent, and if they satisfy a trade-off (Fig. G1, right-hand panels).

Finally, putting together eqs. (G1, G3, G4), we get

$$\mathcal{V}_\alpha^{\text{spec } i} \propto N_i^\alpha \, \tau_i^\nu \propto N_i^{\alpha+\gamma\nu} \approx N_i^{\alpha+\gamma}, \tag{G5}$$

where in the last step we have used that $\nu \approx 1$. The relationship between abundance of perturbed species and community variability is strongly determined by the exponent γ, that is, by the relationship between abundance N_i and response time τ_i. In the case of weak interactions, the latter relationship depends on the assumed link between growth rate r_i and carrying capacity K_i, so that no unambiguous relationship is to be expected between abundance and variability. However, in the limit of strong interactions, we have $\gamma \approx -1$ and

$$\mathcal{V}_\alpha^{\text{spec } i} \propto N_i^{\alpha-1}. \tag{G6}$$

Hence, for immigration-type perturbations ($\alpha = 0$) variability is inversely proportional to the abundance of the perturbed species. In contrast, for environmental perturbations ($\alpha = 2$), variability is directly proportional to the abundance of the perturbed species. These are the relationships depicted in Figs. 4 and 5 of the main text.

8 Variability and abundance statistics

From the observed relationship between abundance and variability (Figs. 4 and 5), patterns for worst- and mean-case variability can be deduced. This reveals a connection between stability and diversity metrics.

Denote by $\mathcal{V}_\alpha^{\text{spec } i}$ the community variability induced by a type-α perturbation fully focused on species i. We start from the power-relationship (G6), linking this variability and the

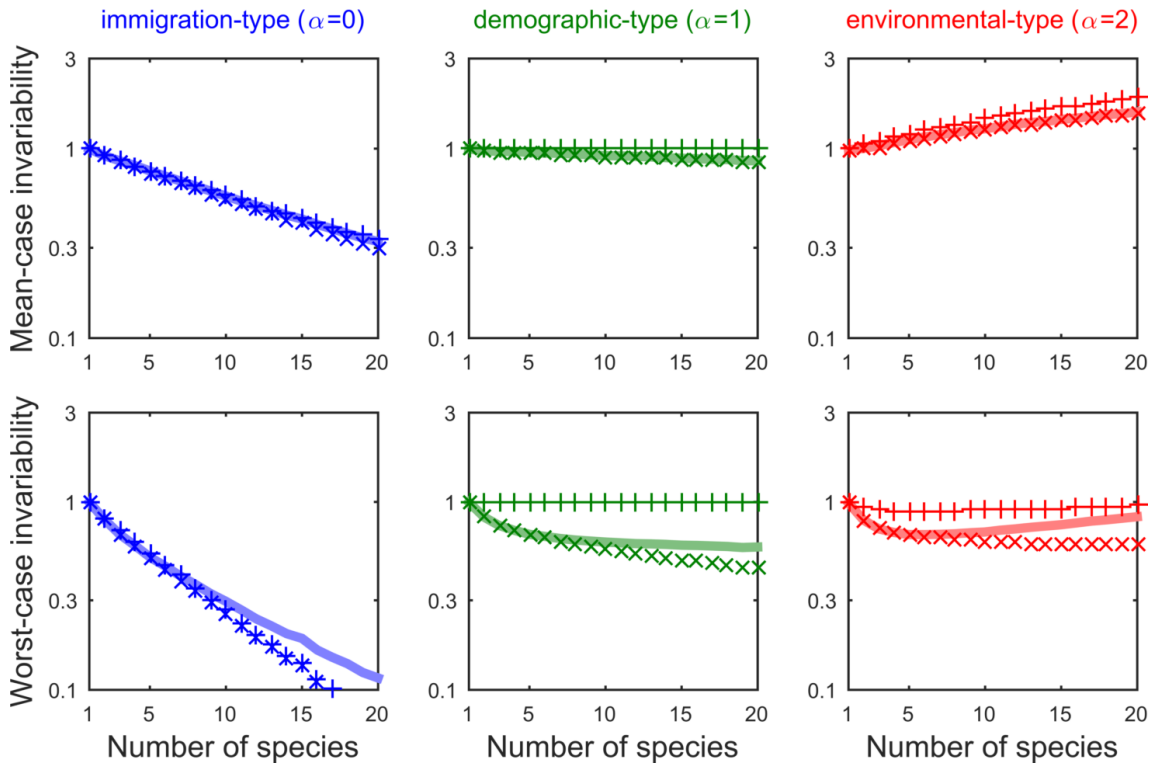

Figure H1: Invariability and species abundance. Top row: mean-case, bottom row: worst-case. $\times$-marks: analytical formula; $+$-marks: approximation in terms of abundance (see Appendix 8); thick line: simulation results. For immigration-type perturbations (first column, in blue), mean-case invariability scales as the harmonic mean abundance (see eq. (H2)), which decreases with diversity. Worst-case invariability scales as the abundance of the rarest species. On the other hand, in response to environmental-type perturbations (third column, in red), mean-case variability scales as the arithmetic mean abundance (see eq. (H4)) so that invariability increases. Worst-case variability scales as the abundance of the most common species. In between (second column, in green), for demographic-type perturbations, neither worst- nor mean-case invariability is determined by statistics of species abundances.

equilibrium abundance of species i. As argued in Appendix 7, we expect this relationship to hold for sufficiently strong interactions.

For immigration-type perturbations ($\alpha = 0$), worst-case variability is approached by taking the maximum over species which gives

$$\mathcal{V}_{\alpha=0}^{\text{worst}} \approx \max_i \mathcal{V}_{\alpha=0}^{\text{spec } i} \propto \frac{1}{\min_i N_i}. \tag{H1}$$

so that the worst case is governed by the rarest species. Because the abundance of the rarest species typically decreases with diversity, the corresponding diversity-stability relationship is decreasing. For mean-case variability, averaging over species individual contributions, we get

$$\mathcal{V}_{\alpha=0}^{\text{mean}} = \frac{1}{S}\sum_i \mathcal{V}_{\alpha=0}^{\text{spec } i} \propto \frac{1}{S}\sum_i \frac{1}{N_i} = \langle N \rangle_{\text{harm}}^{-1}, \tag{H2}$$

where $\langle N \rangle_{\text{harm}}$ stands for the harmonic mean of species abundances. Mean abundance typically decreases with diversity, so that the corresponding diversity-stability relationship is decreasing.

When caused by environmental-type perturbations ($\alpha = 2$), worst-case variability is approached by taking the maximum over species, giving

$$\mathcal{V}_{\alpha=2}^{\text{worst}} \approx \max_i \mathcal{V}_{\alpha=0}^{\text{spec } i} \propto \max_i N_i, \tag{H3}$$

so that the worst case is governed by the most abundant species. For mean-case variability we get

$$\mathcal{V}_{\alpha=2}^{\text{mean}} \propto \frac{1}{S}\sum_i N_i = \langle N \rangle_{\text{arith}}, \tag{H4}$$

the arithmetic mean of species abundances. Mean abundance typically decreases with diver-

sity, so that the corresponding diversity-stability relationship is increasing.

Note that when caused by demographic-type perturbations ($\alpha = 1$) the species-by-species approach does not work: demographic variability probes a collective property of the community. The different relationships between abundance and variability are illustrated in Fig. H1.